



A common lag scenario in quenching of oscillation in coupled oscillators

K. Suresh, S. Sabarathinam, K. Thamilaran, Jürgen Kurths, and Syamal K. Dana

Citation: *Chaos* **26**, 083104 (2016); doi: 10.1063/1.4960086

View online: <http://dx.doi.org/10.1063/1.4960086>

View Table of Contents: <http://scitation.aip.org/content/aip/journal/chaos/26/8?ver=pdfcov>

Published by the [AIP Publishing](#)

Articles you may be interested in

[Synchronization of two memristively coupled van der Pol oscillators](#)

Appl. Phys. Lett. **108**, 084105 (2016); 10.1063/1.4942832

[Practical time-delay synchronization of a periodically modulated self-excited oscillators with uncertainties](#)

Chaos **20**, 043121 (2010); 10.1063/1.3515840

[Effect of common noise on phase synchronization in coupled chaotic oscillators](#)

Chaos **17**, 013105 (2007); 10.1063/1.2424423

[Multi-frequency Oscillations in Coupled Van Der Pol Oscillators](#)

AIP Conf. Proc. **676**, 384 (2003); 10.1063/1.1612274

[Synchronization of driven nonlinear oscillators](#)

Am. J. Phys. **70**, 607 (2002); 10.1119/1.1467909



A common lag scenario in quenching of oscillation in coupled oscillators

K. Suresh,^{1,a)} S. Sabarathinam,^{1,b)} K. Thamilmaran,^{1,c)} Jürgen Kurths,²
 and Syamal K. Dana^{3,4}

¹Center for Nonlinear Dynamics, Bharathidasan University, Trichy 620024, India

²Institute for Physics, Humboldt University, 12489 Berlin, Germany and Potsdam Institute of Climate Impact Research, 14473 Potsdam, Germany

³CSIR-Indian Institute of Chemical Biology, Kolkata 700032, India

⁴Center for Complex System Research Kolkata, Kolkata 700094, India

(Received 29 March 2016; accepted 15 July 2016; published online 3 August 2016)

A large parameter mismatch can induce amplitude death in two instantaneously coupled oscillators. Alternatively, a time delay in the coupling can induce amplitude death in two identical oscillators. We unify the mechanism of quenching of oscillation in coupled oscillators, either by a large parameter mismatch or a delay coupling, by a common lag scenario that is, surprisingly, different from the conventional lag synchronization. We present numerical as well as experimental evidence of this unknown kind of lag scenario when the lag increases with coupling and at a critically large value at a critical coupling strength, amplitude death emerges in two largely mismatched oscillators. This is analogous to amplitude death in identical systems with increasingly large coupling delay. In support, we use examples of the Chua oscillator and the Bonhoeffer-van der Pol system. Furthermore, we confirm this lag scenario during the onset of amplitude death in identical Stuart-Landau system under various instantaneous coupling forms, repulsive, conjugate, and a type of non-linear coupling. *Published by AIP Publishing.* [<http://dx.doi.org/10.1063/1.4960086>]

Oscillation quenching in the form of amplitude death (AD) and oscillation death (OD) is known to appear in oscillatory systems under different coupling schemes. It was first noticed that a large parameter mismatch can induce such a cessation of oscillation in instantaneously coupled oscillators. Later, it was reported that a propagation delay between identical systems can also lead to oscillation quenching. By this time, different coupling schemes, conjugate type, environment coupling, repulsive feedback link, were also found to show the effect of oscillation quenching. We attempt here to unify the onset of oscillation quenching in oscillators under different coupling schemes by a common lag effect that is different from the conventional lag scenario usually seen in mismatched oscillators or in delay system with a mismatch in intrinsic delay. We provide numerical as well as experimental evidence in several paradigmatic model systems.

I. INTRODUCTION

Quenching of oscillation^{1–3} is a well known emergent behavior in coupled oscillators when they drive each other to a stable equilibrium. This was evidenced first as an unexpected silencing of two side-by-side organ pipes⁴ and later demonstrated in chemical oscillators.⁵ This strange phenomenon was, at first, explained^{3,6} as an effect of large parameter mismatch on coupled oscillatory systems. Later, it was also observed in two identical oscillators when a critical propagation delay is introduced in the coupling.^{7,8} Different coupling

forms were later found to be able to induce the quenching of oscillation, namely, dynamical coupling,⁹ conjugate coupling,¹⁰ asymmetric coupling,^{11–13} dynamic environment coupling,¹⁵ nonlinear coupling,¹⁶ quorum sensing coupling,¹⁷ and repulsive coupling link.¹⁸ Two distinct classes of the quenching effects have been identified so far:^{1,2} amplitude death (AD) and oscillation death (OD). In the case of AD, all the coupled oscillators are stabilized to one equilibrium state which may be the origin or any other fixed point. On the other hand, in the case of OD, the coupled systems are stabilized to multiple equilibrium states.

OD originates in coupled systems via diverse bifurcation routes, pitchfork, transcritical, or saddle-node bifurcation^{2,18–21} depending upon the coupling form and the dynamical system. AD usually emerges via reverse Hopf bifurcation (HB) in different systems whatever may be the coupling form.^{1,2} Although AD and OD effects in coupled oscillators are almost well understood, we report here a common lag effect, so far unnoticed, that governs the emergence of AD via a reverse HB in identical or mismatched oscillators under most of the coupling schemes. This lag synchronization (LS) effect first emerges, as usual, in two coupled mismatched oscillators, above a critical coupling; however, the characteristic feature of this lag scenario differs from the conventional LS.¹⁴ We notice this lag scenario first in our experiment on AD in two coupled Chua circuits with a large mismatch. With increasing coupling strength, the coupled Chua circuits undergo a reverse period-doubling from a chaotic state to a period-1 regime. In this period-1 regime, LS is noticed when an increase in the characteristic lag is recorded with the coupling strength, instead of an expected decrease, until a death of oscillation appears at a critically larger lag value. We verify the existence of this lag scenario, in another experiment

^{a)}Electronic mail: ksuresh@cnd.bdu.ac.in

^{b)}Electronic mail: saba.cnd@gmail.com

^{c)}Electronic mail: maran.cnd@gmail.com

with two coupled periodic Bonhoeffer-van der Pol (BVP) oscillators. This lag scenario is analogous to the delay induced AD⁷ in identical oscillators where an increasing conduction delay induces a death above a critical value. We are motivated by these experimental results to address a natural question if the lag effect is a common governing rule of AD in identical or mismatched oscillators irrespective of the coupling forms? We confirm this unknown kind of lag scenario during the onset of AD in identical oscillators under various other coupling forms, namely, repulsive coupling, conjugate coupling, and a type of nonlinear coupling. Basically, we attempt a unification of the phenomenon of quenching of oscillation in coupled oscillators by a common lag effect.

We mention here that a generalized LS (GLS) was reported earlier²⁷ during the onset of AD in two instantaneously coupled delay systems with mismatches in intrinsic delays. AD emerges there at a critically larger mismatch in intrinsic delays at a fixed coupling strength. In contrast, we report a type of GLS that emerges in coupled systems with *a priori* presence of no delay of any form, and more specifically, we focus on an increasing lag effect with coupling that leads to the emergence of AD.

II. LAG SCENARIO: EXPERIMENTAL OBSERVATION

We present our experimental observations for the coupled Chua oscillators and the BVP systems in Figs. 1(a) and 1(b), respectively. We choose two reflection symmetric systems, the 3D Chua oscillator and the 2D BVP oscillator, to check generality of the results. We apply purely diffusive mutual coupling via a resistance between two circuit nodes of both the systems. We consider large parameter mismatch in the oscillators and vary the coupling resistance to observe AD for each coupled system. To our expectation, in both the systems, a LS first emerges where the emergent lag or delay τ (not coupling delay) between the coupled oscillators increases from both left and right in regions I and II, respectively. The intermediate AD regime emerges at critical values of lag at critical R_C values. A difference lies in the coherent relation of the coupled oscillators: for weaker coupling in region I, an anti-LS^{23,24} is observed when the pair of measured time series of the coupled oscillators are out-of-phase (phase difference of 0 to π), while for

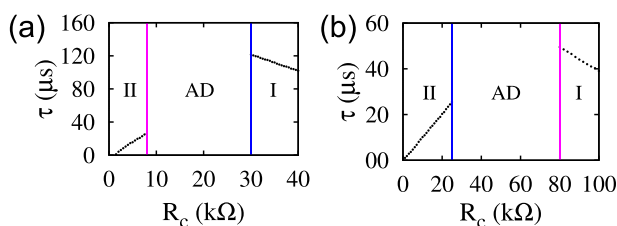


FIG. 1. Emergent lag (τ) as a function of coupling resistance R_C in experiments. AD regimes exist intermediate to two vertical lines, (a) coupled Chua oscillators and (b) coupled Bonhoeffer-van der Pol (BVP) systems. In both systems, in region I at the right side of the AD regime, lag (dotted line) increases with decrease in R_C (increase of coupling strength) and AD emerges for a critical lag τ at a critical R_C . On the left side, in region II, the delay increases with R_C when AD emerges at another critical value. Details of the experiments are presented in supplementary material.²²

stronger coupling in region II, a LS is found as shown in the oscilloscope pictures of time series in Figs. 2(a) and 2(b), respectively. From a visual inspection of the experimental time series of the coupled systems, the lag scenario is not clear, particularly, in the anti-LS regime. However, taking a closer look, we find that it belongs to a more general class of LS, a type of GLS, where the amplitudes of the coupled state variables are not identical although maintained a constant lag. To avoid confusion, the amplitudes are normalized by a scaling constant and compared using a modified similarity measure^{14,25} when the coupled systems are found strongly correlated and emerge with a finite characteristic lag.

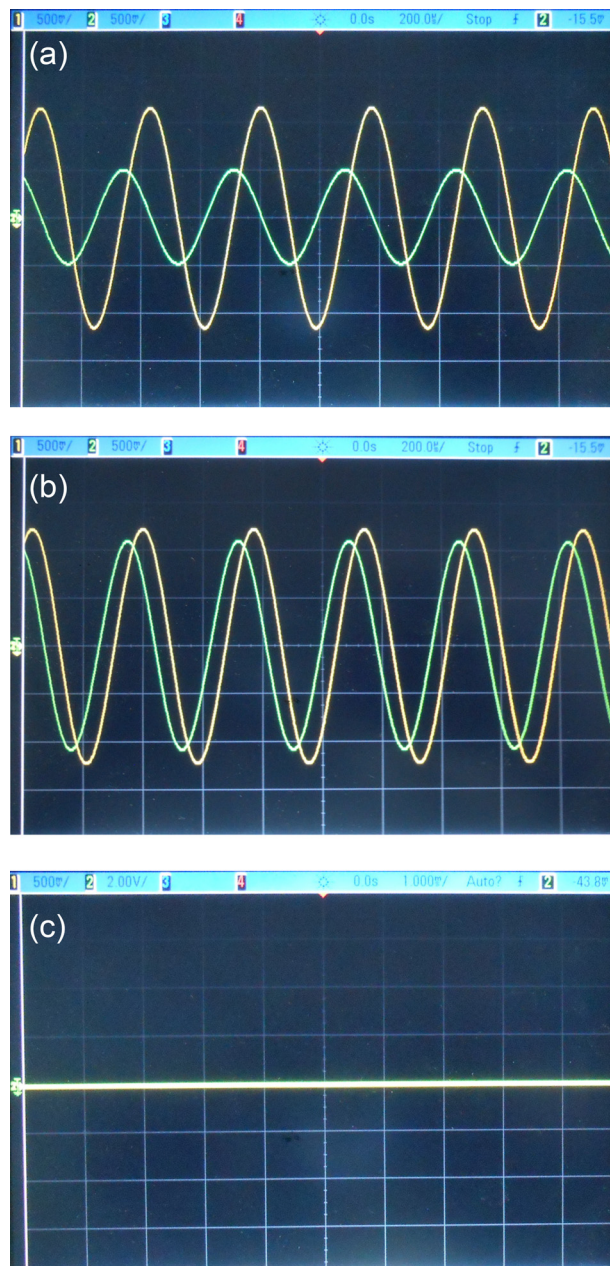


FIG. 2. Oscilloscope pictures of experimental time series of coupled Chua circuits. Measured voltages v_2 and v_4 ²³ plot for (a) $R_C = 32$ k Ω in anti-LS regime, (b) $R_C = 8$ k Ω in LS regime, and (c) $R_C = 20$ k Ω in AD regime as shown in regions I, II, and AD regime, respectively, in Fig. 1(a).

We provide further details of our experiments for both the systems. First, we consider non-identical Chua oscillators with instantaneous diffusive coupling and choose the circuit parameters so that the isolated oscillators are in period-1 regime but with a mismatch of $\Delta f = 142$ Hz. Details of the experimental circuits and their parameters are given in Ref. 22. The coupling resistance R_C is varied when the onset of AD is observed with increasing coupling strength ($1/R_C$). The coupled system develops a quasiperiodic behavior for weak coupling and then becomes period-1 with a little increase of the coupling strength when we start our measurements and data capturing. A similar pair of node voltages v_2 and v_4 (analog of state variables, for details see Ref. 22) of the coupled circuits is captured by the data memory of a digital oscilloscope for each R_C and the lag between them is estimated by using a modified version of the similarity measure^{14,25}

$$S^2(\tau) = \frac{\langle [v_2(t) - \alpha v_4(t - \tau)]^2 \rangle}{[\langle v_2^2(t) \rangle \langle \alpha^2 v_4^2(t) \rangle]^{1/2}}, \quad (1)$$

where $\alpha = v_{2m}/v_{4m}$ is a scaling constant. The v_{2m} and v_{4m} , the maxima of the respective node voltages, are estimated from the measured time series of the coupled oscillators. We modify the standard similarity measure^{25,26} by inserting the scaling or normalizing constant α because the coupled variables show difference in amplitudes (Fig. 2) at a given coupling strength. The measured voltage variable v_2 and the scaled voltage variable αv_4 are now strongly correlated, and it is confirmed by a zero global minimum of the similarity measure $S(\tau)$ at a characteristic lag τ . For a pair of measured time series (v_2, v_4) for each R_C , the global minimum of $S(\tau)$ is obtained with an estimate of its characteristic lag τ . The estimated characteristic lag τ is plotted with R_C in Fig. 1(a), which shows increasing trends for both increasing and decreasing coupling ($1/R_C$) when AD appears for an intermediate coupling range.

This lag effect during the onset of AD is independent of the dynamical system which we confirm by using the second example of the coupled BVP oscillators²² with a large mismatch. We choose this inverse symmetric system, similar to the Chua oscillator, especially, to observe both LS and anti-LS regimes for two extreme values of coupling strength between which the AD appears. In other systems, LS can only be observed during the onset of AD especially if they are identical. Experimental results for the BVP systems are presented in Fig. 1(b) which records an increasing trend of the emergent lag at both ends of the AD regime. The lag between the oscillators increases with the increase/decrease of the coupling strength, and the AD regime sets in for two critical time lags at the two ends. The same procedure, as used for the coupled Chua systems, is followed again to estimate the characteristic lag for different R_C values. Experimental time series of the anti-LS, the LS, and AD are shown in Fig. 3 which correspond to the regions I, II, and the intermediate AD region in Fig. 1(b), respectively. We verify the results in numerical simulations as well and present some details for the coupled Chua oscillator in Sec. III and by the eigenvalue analysis as presented in the supplementary material.²²

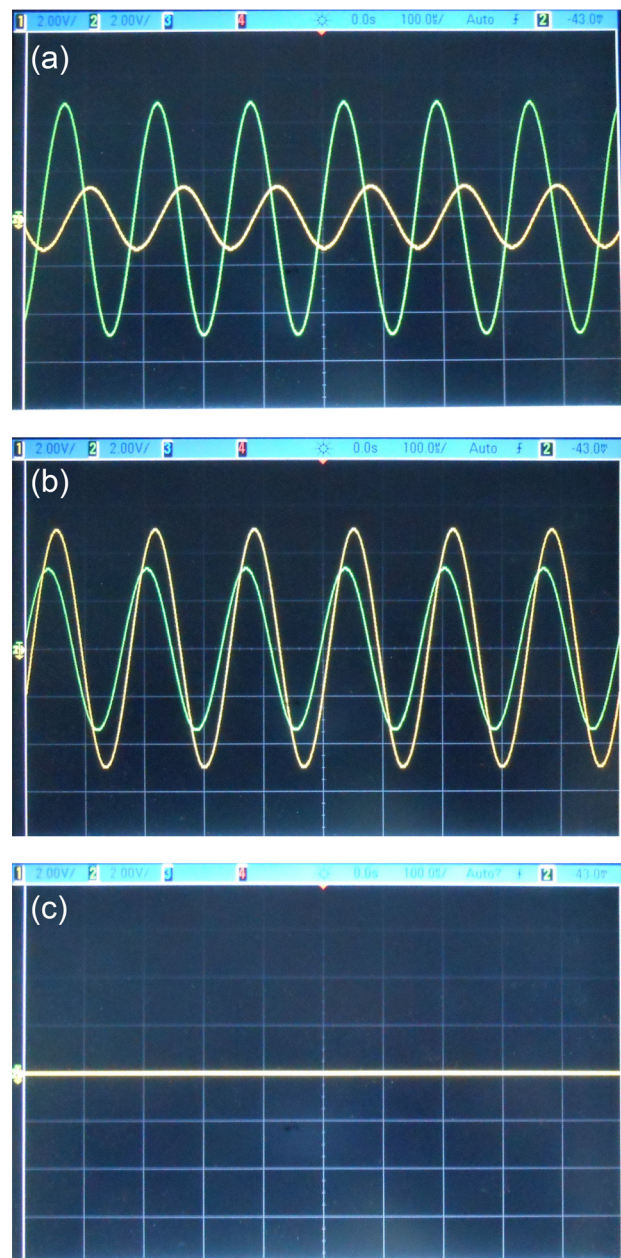


FIG. 3. Oscilloscope pictures of experimental time series of coupled BVP circuits. Measured v_1 and v_2 ²² plot for $R_C = 32$ k Ω in the anti-LS regime (a), $R_C = 8$ k Ω in the LS regime (b), and $R_C = 20$ k Ω in AD regime (c).

III. LAG SCENARIO: NUMERICAL STUDY IN COUPLED CHUA CIRCUIT

We present our numerical results of the lag scenario during the onset of AD in two instantaneously coupled Chua oscillators. The normalized equations of the coupled circuit²² are

$$\begin{aligned} \frac{dx_{1,2}}{dt} &= \alpha_{1,2} [y_{1,2} - x_{1,2} - h(x_{1,2})], \\ \frac{dy_{1,2}}{dt} &= x_{1,2} - y_{1,2} + z_{1,2} + \epsilon_{1,2}(y_{2,1} - y_{1,2}), \\ \frac{dz_{1,2}}{dt} &= -\beta_{1,2}y_{1,2} - \gamma_{1,2}z_{1,2}, \end{aligned} \quad (2)$$

where

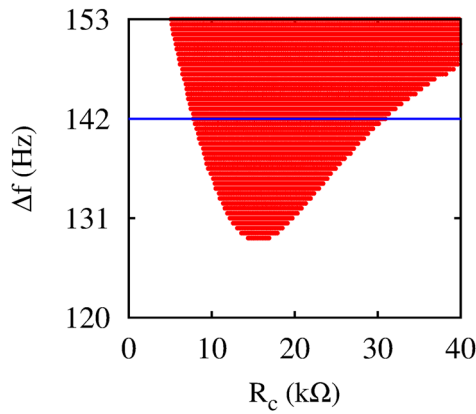


FIG. 4. Phase diagram in the $(R_C - \Delta f)$ space of coupled Chua oscillators. The red region indicates the AD regime. The blue horizontal line corresponds to numerical simulations in Fig. 5.

$$h(x_{1,2}) = b_{1,2}x_{1,2} + 0.5(a_{1,2} - b_{1,2})(|x_{1,2} + 1| - |x_{1,2} - 1|),$$

where $\epsilon_{1,2} = R_{1,2}/R_C$ is the coupling strength. Other parameters are $\alpha_1 = 10.0$, $\alpha_2 = 9.619$, $\beta_1 = 18.05$, $\beta_2 = 16.958$, $a_1 = -1.4402$, $b_1 = -0.7771$, $a_2 = -1.4402$, $b_2 = -0.7771$, $\gamma_1 = 0.209$, and $\gamma_2 = 0.1964$ for resistance values $R_1 = R_2 = 1900\Omega$ in the circuit.²² For the selected parameters, the Chua oscillators both, in isolation, show period-1 limit cycle dynamics with a frequency mismatch of $\Delta f = 142\text{Hz}$. The frequency mismatch is estimated from the frequency-parameter plots of the uncoupled systems.²²

We simulate Eq. (2) for the selected parameters to plot a phase diagram in Fig. 4 and locate the AD regime in the $R_C - \Delta f$ space. It shows a typical Arnold tongue-like structure of the AD regime in the dark region (online red color) which reconfirms the old result, in the literature,^{1,2} that a minimally large Δf is necessary for AD to emerge at a critical R_C value. The AD region widens with Δf having two extrema. The boundary of the AD regime demarcates the contour of the Hopf bifurcation from the oscillatory region.

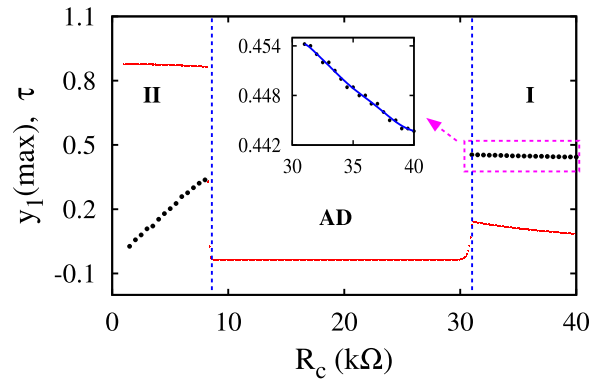


FIG. 5. Maxima of y_1 (red line) as a function of R_C in coupled Chua oscillators. Frequency mismatch = 142 Hz, $R_1 = R_2 = 1900\Omega$. Lag (τ) in black dots between y_1 and y_2 . The inset shows a zoomed version of the lag plot (blue line) at right where back dots are data points.

The horizontal line indicates the selected $(R_C - \Delta f)$ regime of the numerical example presented in Figs. 5 and 6. With increasing coupling strength ($1/R_C$), we hit the boundary of the AD regime at right when an anti-LS is encountered. For larger coupling strength, we reach another boundary at left (smaller R_C) where the oscillation restarts and a LS is now observed. An eigenvalue analysis of the coupled system is done²² to confirm the Hopf bifurcation during the onset of AD at both extremes of R_C .²²

The maxima of numerical time series y_1 in solid lines (red lines) is plotted with R_C in Fig. 5, which becomes zero in the middle (AD regime between two vertical lines). The emergent lag is estimated from the pair of time series (y_1, y_2) using the similarity measure in Eq. (1) and plotted in black dots on both sides of the AD regime. The incremental nature of the lag with coupling strength (decreasing R_C) in region I is clear from a close view of the plot in the inset. At smaller R_C (larger coupling strength), oscillation restarts at the boundary of region II where the lag increases with R_C (decreasing coupling strength) until AD arrives at another

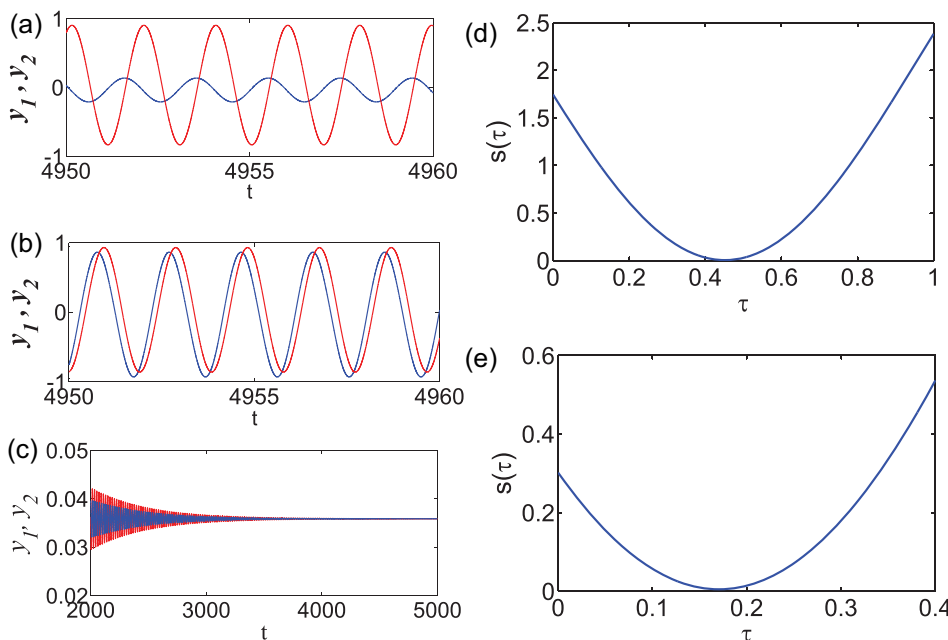


FIG. 6. Numerical results of coupled Chua oscillators. Frequency mismatch $\Delta f = 142\text{Hz}$. Time series of y_1 and y_2 in (a) anti-LS for $R_C = 31.5\text{k}\Omega$, (b) LS for $R_C = 8.2\text{k}\Omega$, and (c) AD regime for $R_C = 20\text{k}\Omega$. The similarity measure $S(\tau)$ shows global minima at critical τ values in (d) anti-LS regime, (e) LS regime.

critical lag value. The time series of the coupled oscillators in the anti-LS, the LS, and the AD regime are shown in Figs. 6(a)–6(c) which correspond to regions I, II, and the AD regime, respectively, in Fig. 5. To confirm the anti-LS and the LS characteristics of the coupled dynamics, the similarity measures of the time series in Figs. 6(a) and 6(b) are plotted in Figs. 6(d) and 6(e), respectively, each showing a strong correlation [$S(\tau)$ shows a global minimum] for a characteristic lag between the scaled variables (y_1 and αy_2) of the coupled systems. In the anti-LS regime,^{23,24} the state variables y_1 and y_2 of the coupled systems are in antiphase but shifted by an additional lag. In this anti-LS regime, y_1 is first inverted, and then, the lag is estimated with αy_2 . Our numerical results thus confirm the lag scenario during the onset of oscillation quenching similar to what is observed in the experiments.

IV. LAG SCENARIO IN IDENTICAL SYSTEMS

Finally, we check the generality of the lag scenario during the onset of AD in coupled identical oscillators. We confirm the effect for three different coupling forms, repulsive, conjugate, and a nonlinear coupling, in two identical Stuart-Landau (SL) oscillators without conduction delay. The paradigmatic SL limit cycle model is, particularly, used here since it is a generic testbed of many dynamical phenomena, including the AD. We mention here that LS is only found in identical systems, no anti-LS is seen at the weaker coupling limit when a phase drifting is only observed. A large parameter mismatch can really induce anti-LS which we do not elaborate since our main target here is to reveal a unique type of lag scenario during the onset of AD and especially explore the effect, if present, in identical systems with no coupling delay. The critical values of AD for all three coupling configurations were already analytically derived earlier.^{10,16,18} However, we are unsuccessful so far to derive analytically the emergent critical lag of AD and, to the best of our knowledge, no such method exists for instantaneously coupled systems although attempts were definitely made in the past.^{28,29}

A. Lag scenario: Repulsive coupling

Quenching of oscillation was reported¹⁸ in coupled SL systems in the presence of additional repulsive coupling. The SL oscillator with repulsive coupling is

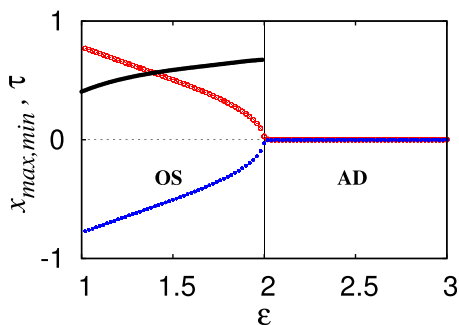


FIG. 7. Numerical results: extrema of x_2 as a function of ϵ in coupled Stuart-Landau oscillators with additional repulsive coupling for $\Delta\omega = 0$ ($\omega_1 = \omega_2 = 3$). The black line is the emergent lag (τ) between x_1 and x_2 .

$$\begin{aligned} \dot{x}_1 &= [1 - (x_1^2 + y_1^2)]x_1 - \omega_1 y_1 + \epsilon(x_2 - x_1), \\ \dot{y}_1 &= [1 - (x_1^2 + y_1^2)]y_1 + \omega_1 x_1, \\ \dot{x}_2 &= [1 - (x_2^2 + y_2^2)]x_2 - \omega_2 y_2 + \epsilon(x_1 - x_2), \\ \dot{y}_2 &= [1 - (x_2^2 + y_2^2)]y_2 + \omega_2 x_2 - \epsilon(y_1 + y_2), \end{aligned} \tag{3}$$

where ϵ is the coupling strength, and $\omega_1 = \omega_2 = \omega = 3$. The attractive diffusive coupling is applied via the x variable, while the repulsive link is applied as a unidirectional negative feedback via the y variable. Figure 7 plots both the maxima and minima of the time series x_2 . The black line shows the emergent delay (τ) between the variables x_1 and x_2 . As usual, the emergent lag is estimated using the similarity measure (Eq. 1) and it increases with coupling strength to a critical value, $\epsilon = \epsilon_c = 2$ when AD sets in.

B. Lag scenario: Conjugate coupling

It is well known¹⁰ that coupling through conjugate variables induces AD in coupled identical oscillators; no coupling delay is necessary. A possible lag scenario was present, as mentioned in Refs. 10 and 26, that leads to the AD; however, it was not elaborated which we confirm here. We consider two identical SL oscillators again with a conjugate coupling

$$\begin{aligned} \dot{x}_1 &= [1 - (x_1^2 + y_1^2)]x_1 - \omega_1 y_1 + \epsilon(y_2 - x_1), \\ \dot{y}_1 &= [1 - (x_1^2 + y_1^2)]y_1 + \omega_1 x_1 + \epsilon(x_2 - y_1), \\ \dot{x}_2 &= [1 - (x_2^2 + y_2^2)]x_2 - \omega_2 y_2 + \epsilon(y_1 - x_2), \\ \dot{y}_2 &= [1 - (x_2^2 + y_2^2)]y_2 + \omega_2 x_2 + \epsilon(x_1 - y_2). \end{aligned} \tag{4}$$

The frequency of the oscillators are taken as $\omega_1 = \omega_2 = \omega = 2$. The maxima and minima of the time series y_1 are given in Fig. 8. The black line shows the emergent lag τ between the conjugate variables y_1 and x_2 . The lag is calculated and seen increasing with coupling strength until it reaches a critical value of $\epsilon_c = 1$ when AD sets in.

C. Lag scenario: Nonlinear coupling

We find a type of nonlinear coupling¹⁶ that induces AD in coupled oscillators. Two identical SL oscillators with a nonlinear coupling are taken

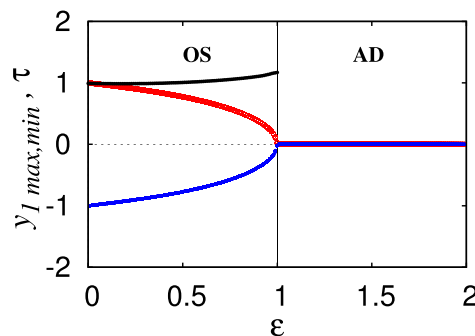


FIG. 8. Numerical results: extrema of y_1 as a function of ϵ in two Stuart-Landau oscillators under conjugate coupling. $\Delta\omega = 0$ ($\omega_1 = \omega_2 = 2$). Black line plots the lag (τ) between the variables y_1 and x_2 .

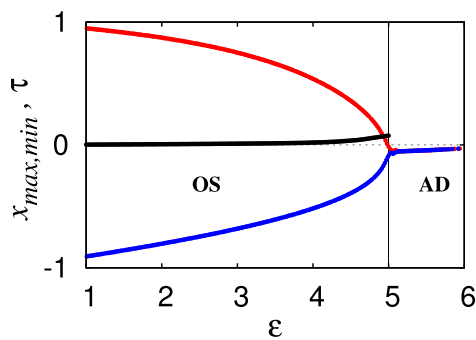


FIG. 9. Numerical result: extrema of y_1 as a function of ϵ in nonlinearly coupled Landau-Stuart oscillators for $\Delta\omega = 0$ ($\omega_1 = \omega_2 = 6$). The black line is the lag (τ) between the variables x_1 and x_2 .

$$\begin{aligned}\dot{x}_1 &= [1 - (x_1^2 + y_1^2)]x_1 - \omega_1 y_1 + \epsilon(x_1 - \alpha) \exp(x_2 - \beta), \\ \dot{y}_1 &= [1 - (x_1^2 + y_1^2)]y_1 + \omega_1 x_1, \\ \dot{x}_2 &= [1 - (x_2^2 + y_2^2)]x_2 - \omega_2 y_2 + \epsilon(x_2 - \alpha) \exp(x_1 - \beta), \\ \dot{y}_2 &= [1 - (x_2^2 + y_2^2)]y_2 + \omega_2 x_2.\end{aligned}\quad (5)$$

The frequency of the oscillators are taken as $\omega_1 = \omega_2 = \omega = 6$ and $\alpha = 1.0$ and $\beta = 0.1$. The maxima and minima of the time series x_1 are shown in the Fig. 9. The black line shows the emergent lag (τ) between the variables x_1 and x_2 , which increases with coupling strength until it increases to a critical value $\epsilon_c = 5$ when AD sets in.

V. DISCUSSION AND SUMMARY

In summary, we identified an unknown kind of lag scenario during the onset of quenching of oscillation in instantaneously coupled identical or mismatched oscillators. This lag scenario has been noticed in both experimental as well as numerical simulations of instantaneously and diffusively coupled mismatched oscillators, the Chua oscillator and the BVP oscillator. In this lag scenario, the mismatched oscillators, as usual, emerge with lag synchronization at a critical coupling strength; however, for a further increase in the coupling strength, instead of usual decrease in the characteristic lag between the coupled systems, it increases. Eventually, the coupled system is stabilized via a reverse Hopf bifurcation at a larger critical lag at a critical coupling. We specifically chose two reflection symmetric systems where a LS in the larger coupling limit and an anti-LS in the weaker coupling limit occurs with an intermediate AD regime. For both the systems, the quenching of oscillation sets in for two different emergent lags at two different critical coupling strengths. In particular, in the weaker coupling regime, we presented a counterintuitive example of anti-LS where the emergent lag time increases with coupling strength until AD emerges at a critically larger lag. This lag scenario is analogous to AD in identical oscillators where an increasing coupling delay stabilizes the system at a critical value. A GLS scenario was reported earlier²⁷ during the onset of AD in delay systems with a mismatch in intrinsic delays; however, the characteristic feature of increasing lag effect during the GLS was not shown there. Especially, we identified this

unknown kind of lag scenario during the onset of AD in identical systems using the paradigmatic SL system under different coupling forms, namely, repulsive feedback, conjugate coupling, and a type of nonlinear coupling. We concluded that a common lag effect (emergent lag or extrinsic coupling delay) governs the onset of quenching of oscillation in coupled oscillators.

ACKNOWLEDGMENTS

K.S. acknowledges the DST, India, and the Bharathidasan University for financial support under the DST-PURSE programme. K.T. acknowledges DST, India, for financial support under Grant No. SR/S2/HEP-015/2010. S.K.D. was supported by the CSIR (India) Emeritus scientist scheme.

- ¹G. Saxena, A. Prasad, and R. Ramaswamy, *Phys. Rep.* **521**, 205 (2012).
- ²A. Koseska, E. Volkov, and J. Kurths, *Phys. Rep.* **531**, 173 (2013).
- ³D. G. Aronson, G. B. Ermentrout, and N. Kopell, *Physica D* **41**, 403 (1990); G. B. Ermentrout and N. Kopell, *SIAM J. Appl. Math.* **50**, 125 (1990).
- ⁴J. W. S. Rayleigh, *The Theory of Sound* (Dover Publications, 1945), Vol. 2; M. Abel, K. Ahnert, and S. Bergweiler, *Phys. Rev. Lett.* **103**, 114301 (2009).
- ⁵K. Bar-Eli, *Physica D* **14**, 242 (1985); M. F. Crowley and I. R. Epstein, *J. Phys. Chem.* **93**, 2496 (1989).
- ⁶P. C. Matthews and S. H. Strogatz, *Phys. Rev. Lett.* **65**, 1701 (1990); P. C. Matthews, R. E. Mirollo, and S. H. Strogatz, *Physica D* **52**, 293 (1991).
- ⁷D. V. Raman Reddy, A. Sen, and G. L. Johnston, *Phys. Rev. Lett.* **80**, 5109 (1998).
- ⁸A. Prasad, *Phys. Rev. E* **72**, 056204 (2005); A. Prasad, J. Kurths, S. K. Dana, and R. Ramaswamy, *Phys. Rev. E* **74**, 035204(R) (2006).
- ⁹K. Konishi, *Phys. Rev. E* **68**, 067202 (2003).
- ¹⁰R. Karnatak, R. Ramaswamy, and A. Prasad, *Phys. Rev. E* **76**, 035201 (2007).
- ¹¹M. Yoshimoto, K. Yoshikawa, and Y. Mori, *Phys. Rev. E* **47**, 864 (1993).
- ¹²O. Popovych, Y. Maistrenko, E. Mosekilde, A. Pikovsky, and J. Kurths, *Phys. Rev. Lett.* **275**, 401 (2000).
- ¹³S. Yanchuk, Y. Maistrenko, and E. Mosekilde, *Physica D* **154**, 26 (2001).
- ¹⁴M. G. Rosenblum, A. S. Pikovsky, and J. Kurths, *Phys. Rev. Lett.* **78**, 4193 (1997); O. V. Sosnovtseva, A. G. Balanov, T. E. Vadivasova, V. V. Astakhov, and E. Mosekilde, *Phys. Rev. E* **60**, 6560 (1999); S. Taherion and Y. C. Lai, *ibid.* **59**, R6247 (1999); S. Boccaletti and D. L. Valladares, *ibid.* **62**, 7497 (2000); P. K. Roy, S. Chakraborty, and S. K. Dana, *Chaos* **13**, 342 (2003).
- ¹⁵V. Resmi, G. Ambika, and R. E. Amritkar, *Phys. Rev. E* **84**, 046212 (2011).
- ¹⁶A. Prasad, M. Dhamala, B. M. Adhikari, and R. Ramaswamy, *Phys. Rev. E* **81**, 027201 (2010).
- ¹⁷A. Koseska, E. Volkov, and J. Kurths, *Chaos* **20**, 023132 (2010); E. Ullner, A. Zaikin, E. Volkov, and J. Garcia-Ojalvo, *Phys. Rev. Lett.* **99**, 148103 (2007).
- ¹⁸C. R. Hens, P. Pal, O. I. Olusola, and S. K. Dana, *Phys. Rev. E* **88**, 034902 (2013); C. R. Hens, P. Pal, P. K. Roy, A. Sen, and S. K. Dana, *ibid.* **89**, 032901 (2013); Bidish K. Bera, Chittaranjan Hens, and Dibakar Ghosh, *Phys. Letts. A* **380**, 2366 (2016).
- ¹⁹J. J. Suárez-Vargas, J. A. González, A. Stefanovska, and P. V. E. McClintock, *Euro. Phys. Lett.* **85**, 38008 (2009).
- ²⁰A. Koseska, E. Volkov, and J. Kurths, *Phys. Rev. Lett.* **111**, 024103 (2013).
- ²¹N. F. Rulkov, M. M. Suschik, L. S. Tsimring, and H. D. I. Abarbanel, *Phys. Rev. E* **51**, 980 (1995).
- ²²See supplementary material at <http://dx.doi.org/10.1063/1.4960086> for the circuit schematics of the coupled Chua oscillator and the coupled BVP oscillator are given with component values. Experimental details are described. The normalization of the dynamical equations are made. Details of numerical results of the coupled BVP oscillator is presented.
- ²³D. Ghosh, I. Grosu, and S. K. Dana, *Chaos* **22**, 033111 (2012).

- ²⁴M. Lakshmanan and D. V. Senthilkumar, *Dynamics of Nonlinear Time Delay Systems* (Springer, 2010).
- ²⁵S. K. Dana, B. Blasius, and J. Kurths, *Chaos* **16**, 023111 (2006).
- ²⁶W. Zou, X. G. Wang, Q. Zhao, and M. Zhan, *Front. Phys. China* **4**, 97 (2009).
- ²⁷T. Banerjee and D. Biswas, *Chaos* **23**, 043101 (2013).
- ²⁸N. J. Corron, J. N. Blakely, and S. D. Pethel, *Chaos* **15**, 023110 (2005).
- ²⁹C.-U. Choe, T. Dahms, P. Hoewel, and E. Schöll, *Phys. Rev. E* **81**, 025205 (2010).